

## Freeze-thaw cycles alter the growth sprouting strategy of wetland plants by promoting denitrification

Shanshan Ding<sup>1,2</sup>, Yuanchun Zou<sup>3</sup>  & Xiaofei Yu<sup>1,2,3</sup>  

Freeze-thaw cycles exert an important abiotic stress on plants at the beginning of winter and spring in mid-to-high latitudes. Here, we investigate whether the effects of freeze-thaw cycles are carried over into the growing season in wetlands. We conduct a temperature-controlled experiment under two freeze-thaw and two flooding conditions on a typical plant (*Scirpus planiculmis*) and soil from the Momoge wetland (China) and analyze the microbial nitrogen metabolism, based on metagenomic sequencing. We show that freeze-thaw cycles earlier in the year significantly inhibit plant sprouting and early growth. Specifically, they promote denitrification and thus reduce nitrogen levels, which in turn intensifies nitrogen limitation in the wetland soil. We find that plants tend to sprout later but faster after they are exposed to freeze-thaw cycles. Wetland flooding could alleviate these medium-term effects of freeze-thaw cycles. Our results suggest that wetland plants in mid-to-high latitudes have evolved sprouting and growth strategies to adapt to climatic conditions at the beginning of winter and spring.

<sup>1</sup>Engineering Research Center of Low-Carbon Treatment and Green Development of Polluted Water in Northeast China, Ministry of Education & State Environmental Protection Key Laboratory for Wetland Conservation and Vegetation Restoration, School of Environment, Northeast Normal University, 130117 Changchun, China. <sup>2</sup>Key Laboratory of Vegetation Ecology of Ministry of Education & Key Laboratory of Geographical Processes and Ecological Security of Changbai Mountains, Ministry of Education, School of Geographical Sciences, Northeast Normal University, 130024 Changchun, China. <sup>3</sup>Heilongjiang Xingkai Lake Wetland Ecosystem National Observation and Research Station & Key Laboratory of Wetland Ecology and Environment & Jilin Provincial Joint Key Laboratory of Changbai Mountain Wetland and Ecology, Northeast Institute of Geography and Agroecology, Chinese Academy of Sciences, 130102 Changchun, China. ✉email: [yuxf888@nenu.edu.cn](mailto:yuxf888@nenu.edu.cn)

In recent decades, the air temperature of northern ecosystems in winter and spring has increased more than in summer and the global mean, and the trend will continue<sup>1</sup>. The increasing air temperature, as the key environmental factor in winter, will alter the soil's frozen and freeze-thaw situations. In total, 20–50% of soil carbon and nitrogen cycling occurs during winter<sup>2</sup>, and greenhouse gas emissions contribute more than 50% of the total annual emissions due to pulse emissions during freeze-thaw periods<sup>3</sup>. Thus, soil freeze-thaw greatly influences ecosystem processes and functions, which cannot be ignored on the inter-annual scale<sup>4</sup>. The real influences of freeze-thaw on ecosystems, however, have yet to be revealed because we have a limited understanding of how plants, soil, and microbial communities change after the freeze-thaw period.

Substantial efforts have been made to investigate the freeze-thaw's ecological effects under climate change. Numerous studies have focused on the freeze-thaw's immediate effects on soil biogeochemical cycles, with sampling occurring during or at the end of the freeze-thaw period, proving that freeze-thaw causes substantial carbon and nitrogen release<sup>5,6</sup>. Studies of the freeze-thaw's immediate effects on plants have focused on the responses of plant performance in various ecosystems, such as farmland, the arctic, the alpine, and the forest, and have found that the freeze-thaw could cause root injury or mortality<sup>7</sup>, change osmotic adjustment and antioxidant defense systems<sup>8</sup>, and obviously decrease photosynthesis<sup>9</sup>. Additionally, far less research has been undertaken to study the freeze-thaw's carry-over effects than the immediate effects, despite evidence that the freeze-thaw's carry-over effects changed carbon and nitrogen processes for months to years<sup>10,11</sup>. For example, the freeze-thaw's carry-over effects altered respiration, mineralization, and root turnover (root production and fine root length) of the subsequent growing season<sup>12,13</sup> it could even change the plant productivity and relative species abundance of grasses and forbs over multiple growing seasons<sup>14</sup>. However, these investigations are far from sufficient for our knowledge of the freeze-thaw's carry-over effects because they mostly proved the existence of carry-over effects but did not provide a clear exposition of the mechanism. Furthermore, these studies focused on soil biogeochemical processes, root turnover, and plant productivity<sup>14–16</sup> but neglected the responses of plant sprouting and early growth in the early growing season, although this stage is critical for plant survival, growth, and fitness<sup>17,18</sup>.

Additionally, the freeze-thaw's carry-over effects on ecosystems might be complex. A previous study indicated that the freeze-thaw's impacts on plant nitrogen uptake might be offset by soil warming in the growing season<sup>19</sup>. The freeze-thaw cycles are accompanied by soil temperature fluctuations and hydrological changes resulting from warmer air temperatures and snow melting<sup>1</sup>. Conditions, including warmer temperatures, soil moisture, and substrate supply, are thought to be important during the shoulder season because they promote microbial metabolism, which in turn provides nutrients for plant growth in the subsequent season<sup>20</sup>. Therefore, other environmental factors may act on the processes influenced by the freeze-thaw's carry-over effects, further disturbing the freeze-thaw's carry-over effects.

Wetlands are important terrestrial carbon and nitrogen pools<sup>21</sup> and are among the most vulnerable ecosystems to climate change<sup>22</sup>. Boreal wetlands are susceptible to soil freeze-thaw<sup>23</sup> where plant litter decomposition during frozen and freeze-thaw periods accounts for more than half of the annual decomposition<sup>24</sup>. Seasonal freeze-thaw generally occurs during the shoulder seasons of winter-spring and autumn-winter, influencing wetland soils deeper than 90 cm<sup>25</sup>. During freeze-thaw periods, complex physical, chemical, and biological changes

take place in wetland soil, including fragmentation of soil aggregates<sup>26</sup>, emission of greenhouse gases<sup>27</sup>, sorption of soil nutrients<sup>28</sup>, and changes in activity, community composition, and functions of soil microorganisms<sup>29,30</sup>, all of which result in considerable changes in wetland functions and processes. Similar to the studies mentioned above, studies in wetlands neglected to investigate the freeze-thaw's carry-over effects. Additionally, winter climatic conditions have carry-over effects on the hydrological cycle in spring and summer<sup>1</sup>. Therefore, hydrological conditions, which are extremely critical for a wetland's structure and function<sup>31</sup>, might alleviate or intensify the freeze-thaw's carry-over effects. Therefore, the scientific questions in this study are as follows: (1) Do freeze-thaw cycles have carry-over effects on wetland soil nutrients in the early growing season? What is the related microbial mechanism? (2) Do freeze-thaw cycles have carry-over effects on wetland plant sprouting and early growth? What are the wetland plant adaptation strategies? Three main outcomes of the study are: (1) Freeze-thaw's carry-over effects strengthened denitrification and resulted in soil nitrogen reduction, thereby enhancing wetland nitrogen limitation and inhibiting plant sprouting and seedling growth. (2) Wetland plant adjusted its sprouting strategies to adapt to the enhanced nitrogen limitation. (3) Flooding could alleviate the freeze-thaw's carry-over effects.

## Results

**The carry-over effects of freeze-thaw on plant sprouting and early growth.** In this study, we used *Scirpus planiculmis* (*S. planiculmis*, a typical wetland plant) and soil from the Momoge wetland to conduct a temperature-controlling simulation experiment under two freeze-thaw conditions (freeze-thaw: F, control: NF) and two flooding conditions (0 cm: non-flooding, 10 cm: flooding) to resolve the scientific questions mentioned above, and their interaction effects were also explored (0 cm. F: non-flooding × freeze-thaw; 0 cm. NF: non-flooding × control; 10 cm. F: flooding × freeze-thaw; 10 cm. NF: flooding × control).

**Sprouting phase:** The sprouting number in the freeze-thaw groups was less than that in the control group during the whole experimental period. The sprouting number under non-flooding conditions was significantly less and more than that under flooding conditions at the early sprouting period (first 7 days) and day 21, respectively (Fig. 1a, c and Supplementary Table 1). The sprouting number followed a trend of 0 cm. F < 0 cm. NF < 10 cm. F < 10 cm. NF at the early sprouting period, and 10 cm. NF < 10 cm. F < 0 cm. F < 0 cm. NF on day 21. We found there were interaction influences between flooding conditions and the freeze-thaw's carry-over effects on the day 3, day 7, day 14, and day 21 (Fig. 1e). The sprouting speed was inhibited by the freeze-thaw's carry-over effects, but promoted by the flooding conditions before day 7 (Fig. 1b, d and Supplementary Table 1). Additionally, the interaction effects existed on day 3, day 6, and day 21 (Fig. 1f). Moreover, the freeze-thaw's carry-over effects on the sprouting number and speed were greater under the non-flooding conditions than under the flooding conditions. According to the nonlinear curve fit results, plants showed a later but faster sprouting-time pattern under the freeze-thaw's carry-over effects (Fig. 5b, c and Supplementary Table 6).

**Early growth phase:** The number of ramets (a height of over 10 cm, a green appearance), leaf number, height, maximum photochemical quantum yield of photosystem II (Fv:Fm), leaf width, and aboveground biomass were significantly decreased by flooding, whereas stem diameter and stem: leaf ratio (S:L ratio) were significantly increased by flooding. The Fv:Fm was significantly decreased by the carry-over effects of freeze-thaw. In addition, the number of ramets, leaf number, and height were

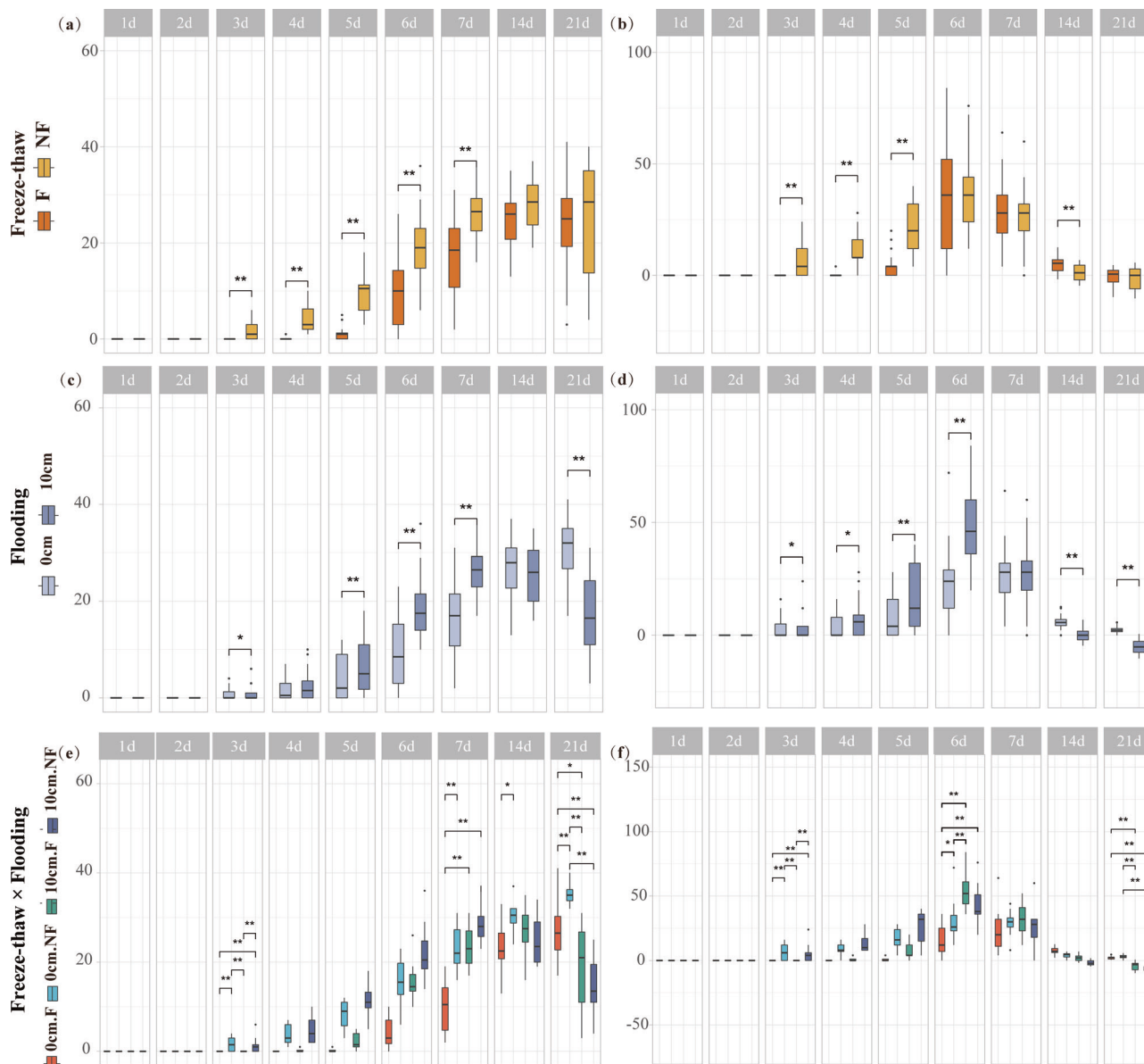


**Fig. 1 Plant sprouting responses to the carry-over effects of freeze-thaw under different flooding conditions.** Five summary statistics are shown in one box plot: The center line indicates the median value, the lower and upper hinges the 25th and 75th percentiles, and the lower and upper whiskers the minimum and maximum of 1.5 times the interquartile range. Furthermore, the dots in box plots denote samples that are outside of 1.5 times the interquartile range. Post hoc analysis was performed when interaction effects existed between freeze-thaw and flooding. **(a, c, e)** Sprouting number; **(b, d, f)** sprouting speed (% day<sup>-1</sup>); \*\**p* < 0.01; \**p* < 0.05; 0 cm: non-flooding; 10 cm: flooding; F: freeze-thaw treatment; NF: control; 0 cm. F: non-flooding × freeze-thaw; 0 cm. NF: non-flooding × control; 10 cm. F: flooding × freeze-thaw; 10 cm. NF: flooding × control.

also influenced by the interaction effects of the freeze-thaw’s carry-over effects and flooding, which showed a similar trend with sprouting number on day 21 (10 cm.NF < 10 cm.F < 0 cm.F < 0 cm.NF; mentioned above). The changes in the number of ramets and leaf number showed the freeze-thaw’s carry-over effects were greater under non-flooding conditions than under flooding conditions (Supplementary Fig. 2). The contents of total carbon (TC) in leaves, total phosphorus (TP) in stems, and total sulfur (TS) in stems were significantly decreased by the freeze-thaw’s carry-over effects, whereas total nitrogen (TN) in stems, TP in stems, TS in leaves, and TS in stems were significantly increased by flooding and TC in leaves was decreased by flooding (Supplementary Fig. 3). In addition, for most plant traits, the effect size analysis revealed that the influence direction of freeze-thaw’s carry-over effects was opposite to that of

flooding, and the interaction effects were weaker than freeze-thaw’s carry-over effects or flooding effects (Supplementary Fig. 11).

**Soil temperature changes during the freeze-thaw period and the carry-over effects of freeze-thaw on soil nutrients.** During the freeze-thaw processes, we recorded the soil temperature at a depth of 5 cm. The maximum, minimum, and mean temperatures in one freeze-thaw cycle under 0 cm.F were lower than those under other conditions, and the freezing duration was longer. Compared with non-flooding conditions, soil temperatures under flooding conditions showed fewer differences between freeze-thaw and control groups (Supplementary Fig. 4 and Supplementary Table 3).

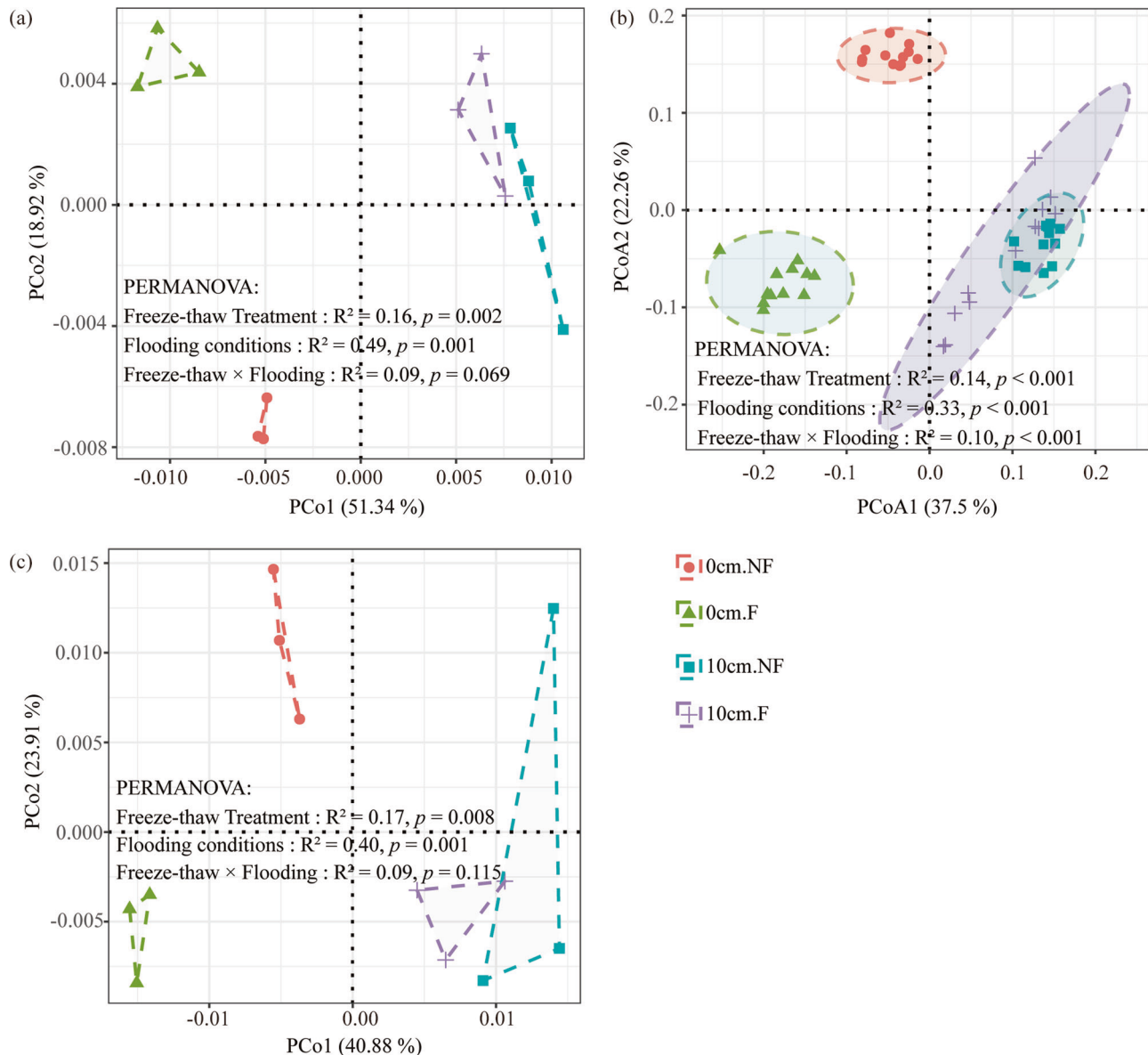


**Fig. 2 Responses of beta diversity of microbial community and functions to the carry-over effects of freeze-thaw under flooding conditions.** **a** PCoA results of N-cycling functional genes; **b** PCoA results of microbial community composition based on OTU, shadings represent 95% confidence ellipses for groups; **c** PCoA results of denitrification functional genes; 0 cm. F: non-flooding  $\times$  freeze-thaw; 0 cm. NF: non-flooding  $\times$  control; 10 cm. F: flooding  $\times$  freeze-thaw; 10 cm. NF: flooding  $\times$  control.

Soil nitrogen, including TN, total organic nitrogen (TON),  $\text{NO}_3^-$ -N,  $\text{NH}_4^+$ -N, and N:P ratio, was decreased by the freeze-thaw's carry-over effects and increased by flooding (Supplementary Fig. 5). Furthermore, the sizes of the interaction effects on soil nitrogen were the lowest (Supplementary Fig. 11). The freeze-thaw's carry-over effects on  $\text{NO}_3^-$ -N under the non-flooding conditions were greater than those under the flooding conditions, and  $\text{NO}_3^-$ -N under 0 cm.F treatment was significantly lower than that under the other treatments ( $p < 0.01$ ). The TC was significantly increased by flooding ( $p < 0.01$ ) but was not influenced by the carry-over effects of freeze-thaw. The TP was not influenced by any experimental factor.

**The carry-over effects of freeze-thaw on microbial community attributes.** For alpha diversity, Simpson's diversity index of operational taxonomic units (OTU) was significantly increased by

the flooding conditions and decreased by the freeze-thaw's carry-over effects, whereas N-cycling genes had conversely changed trends with OTU (Supplementary Fig. 6). Simpson's diversity index of OTU under 0 cm.F treatment was significantly lower than that under the other treatments ( $p < 0.01$ ), and the freeze-thaw's carry-over effects on the alpha diversity of the microbial community under the non-flooding conditions were greater than those under the flooding conditions. Similar to soil nitrogen, the effect sizes of interactions on Simpson's diversity index of OTU and N-cycling genes were the smallest (Supplementary Fig. 11). For beta diversity, the soil microbial community under the freeze-thaw's carry-over effects and flooding conditions showed a consistent changing trend with soil microbial functions (Fig. 2). The principal coordinate analysis (PCoA) results showed obvious separation between 0 cm.F and 0 cm.NF, and no obvious separation between 10 cm.F and 10 cm.NF. Furthermore, for soil microbial functions, the permutation multivariate analysis of

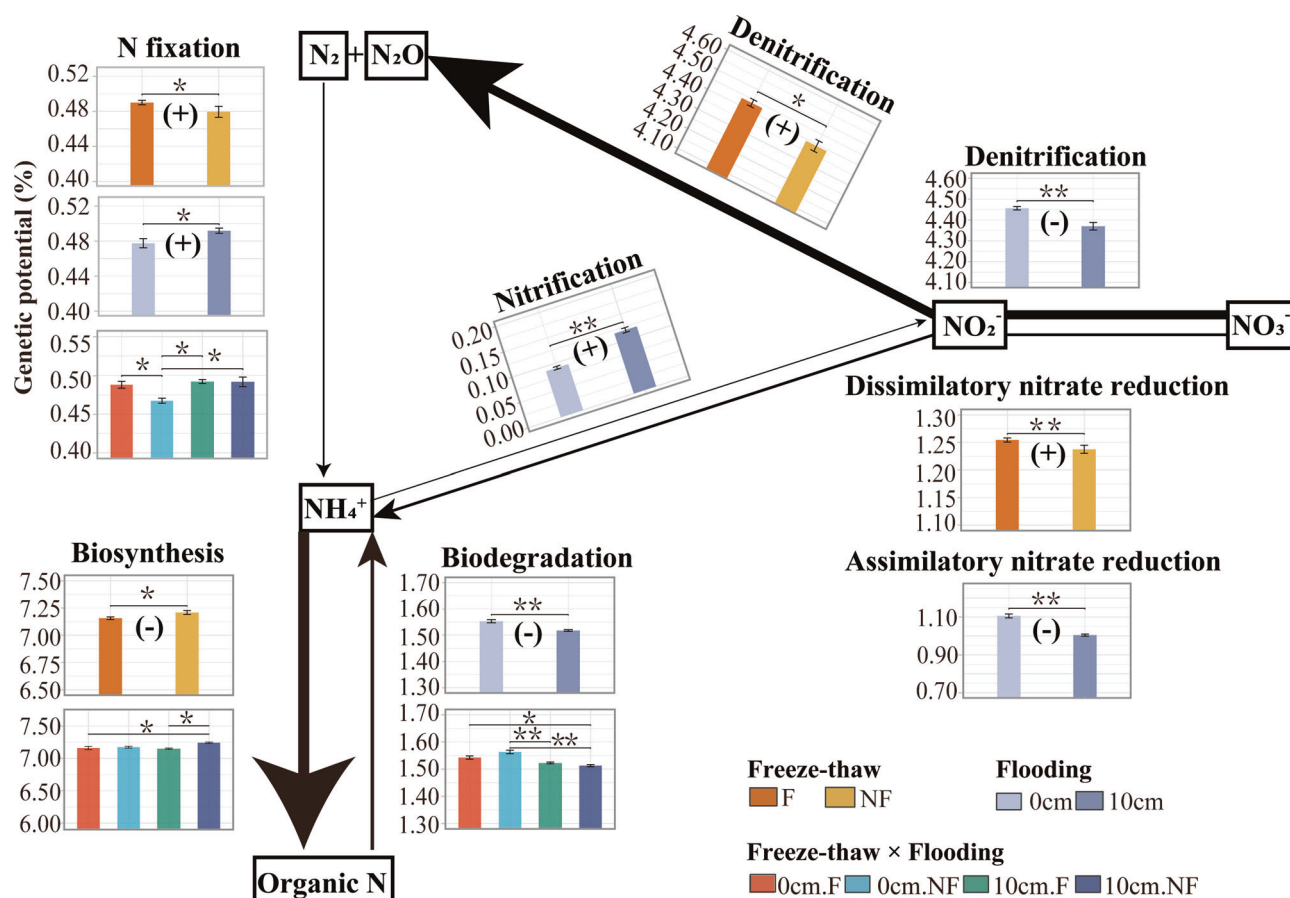


**Fig. 3 Nitrogen cycle pathways in wetland soils with varied treatments.** Arrow sizes are proportional to the genetic potential for metabolic processes. Bar plots are the genetic potential of N-cycling metabolic processes which were calculated using the relative abundance of N-cycling functional genes. “+” indicates that the genetic potential significantly increased under flooding or the carry-over effect of freeze-thaw, and “-” indicates a decrease. Metabolic processes with significant differences under flooding conditions and the carry-over effects of freeze-thaw are shown. \*\* $p < 0.01$ ; \* $p < 0.05$ ; error bars denote SE (freeze-thaw:  $n = 6$ ; flooding:  $n = 6$ ; freeze-thaw × flooding:  $n = 3$ ); 0 cm: non-flooding; 10 cm: flooding; F: freeze-thaw treatment; NF: control; 0 cm. F: non-flooding × freeze-thaw; 0 cm. NF: non-flooding × control; 10 cm. F: flooding × freeze-thaw; 10 cm. NF: flooding × control.

variance (PERMANOVA) results showed that only significant differences existed between freeze-thaw and control groups, as well as between the flooding and non-flooding groups (Fig. 2a, c). For the soil microbial community, the PERMANOVA results showed that significant differences existed between different treatments, except between 10 cm.F and 10 cm.NF (Fig. 2b and Supplementary Table 2).

To determine the differentially abundant microorganisms, the linear discriminant analysis effect size (LEfSe) analysis was performed between different treatments (Supplementary Fig. 7). At the phylum level, *Proteobacteria*, *Chloroflexi*, *Firmicutes*, *Bacteroidetes* and *Gemmatimonadetes* were the differentially abundant microorganisms. Furthermore, *Proteobacteria*, *Chloroflexi*, *Firmicutes*, *Bacteroidetes*, and *Gemmatimonadetes* belonged to the top 10 most abundant microorganisms at the phylum level (Supplementary Fig. 8), and the sums of their relative abundance reached 77.79% (0 cm.F), 76.21% (0 cm.NF), 74.63% (10 cm.F), and 73.47% (10 cm.NF), respectively.

For the changes in N-cycling metabolism processes (Fig. 3; Supplementary Fig. 9), the genetic potential of biosynthesis, denitrification, and biodegradation were the main metabolic processes. N fixation, denitrification, and dissimilatory nitrate reduction were significantly enhanced by the freeze-thaw’s carry-over effects, whereas biosynthesis was significantly weakened by the freeze-thaw’s carry-over effects. In addition, N fixation and nitrification were significantly enhanced by flooding, whereas

assimilatory nitrate reduction, biodegradation, and denitrification were significantly weakened by flooding. Moreover, the freeze-thaw’s carry-over effects on N fixation under the non-flooding conditions were greater than those under the flooding conditions. Similar to plant traits, soil nutrients, and microbial alpha diversity, the interaction effects on the genetic potential of N-cycling processes were the lowest (Supplementary Fig. 11).

### Relationships among plant eco-physiological characteristics, soil nutrients and soil microbial community attributes.

The soil microbial community attributes were correlated with soil nutrients and plant eco-physiological characteristics according to the Spearman correlation and partial Mantel test (Supplementary Fig. 10). In addition, plant sprouting and early growth were also correlated with soil nutrients to various degrees. The distance-based redundancy analysis (db-RDA) and variance partitioning analysis (VPA) (Fig. 4) results showed that the genetic potential of denitrification was the dominant factor controlling the changes in soil nitrogen and explaining 79% of the variation. Furthermore, the structural equation model (SEM) results showed that denitrification controlled the soil nitrogen and indirectly influenced plant sprouting and early growth (Fig. 5a).

### Discussion

**Freeze-thaw has carry-over effects on enhancing denitrification and resulting in a reduction in soil nitrogen.** In this study, the

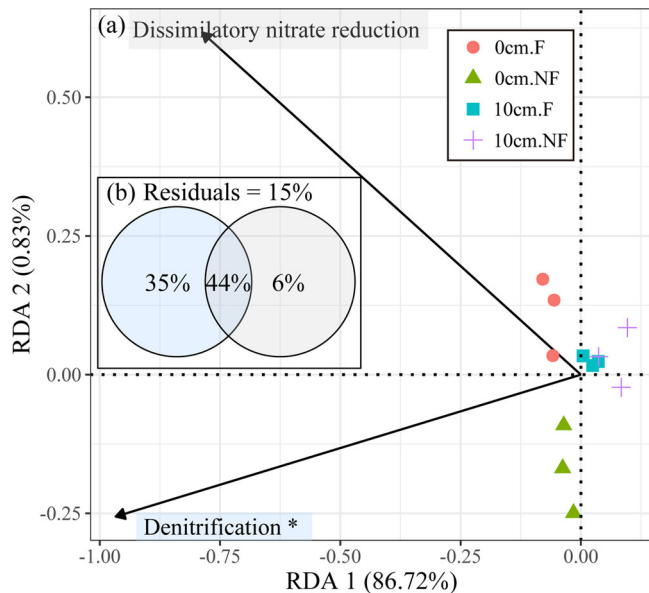


**Fig. 4** The db-RDA and VPA results regarding the influence of N-cycling metabolic processes on soil nitrogen. **a** The db-RDA result; **b** the VPA result; asterisk indicates the significant influence of metabolic processes on soil nitrogen content; the blue shadow indicates denitrification; the gray shadow indicates dissimilatory nitrate reduction; the numbers in the subplot **b** indicate the explained variance of different N-cycling metabolic processes on soil nitrogen; 0 cm. F: non-flooding × freeze-thaw; 0 cm. NF: non-flooding × control; 10 cm. F: flooding × freeze-thaw; 10 cm. NF: flooding × control.

freeze-thaw groups had lower soil nitrogen than the control groups in the early growing season, whereas earlier research on the immediate effects of freeze-thaw revealed that the freeze-thaw groups had higher contents of  $\text{NH}_4^+\text{-N}$  and  $\text{NO}_3^-\text{-N}$  than the control groups during the freeze-thaw period<sup>13,21,32</sup>. Therefore, the freeze-thaw's carry-over effects on soil nitrogen are in the opposite direction from the freeze-thaw's immediate effects, which could be attributed to the freeze-thaw's continuous enhancement of denitrification and insignificant influences of nitrification and mineralization (Fig. 3 and Supplementary Figs. 9 and 11). We also found that the diversity of denitrification functional genes differed significantly between the freeze-thaw and control groups (Fig. 2c). Compared to the carry-over effects, the freeze-thaw's immediate effects increase the soil nitrogen during freeze-thaw period through enhancing nitrification and mineralization, breaking the aggregates, and lysing microorganisms<sup>21,33</sup>. One of the reasons that freeze-thaw continuously enhances denitrification could be the release of soil inorganic nitrogen. Additionally, the freeze-thaw's immediate effects have greater effects on nitrification and mineralization than on denitrification<sup>34</sup>, providing a substantial reaction substrate and further improving denitrification after the freeze-thaw. According to the db-RDA and VPA results, only denitrification among N-cycling metabolic processes significantly altered soil nitrogen and explained 79% of the variation (Fig. 4). The SEM results further verified the abovementioned explanations and demonstrated the denitrification–soil nitrogen cascade relationship under the freeze-thaw's carry-over effects (Fig. 5a). In addition, the TN in leaves decreased in the freeze-thaw group, which could also demonstrate the carry-over effects of freeze-thaw on wetland soil nitrogen, as N concentrations in leaves decreased with decreasing N availability<sup>35</sup>. Moreover, the N:P ratio in plant leaves was less than 14 in this study (Supplementary Fig. 2), indicating that the soil used for this experiment came

from an N-limited ecosystem<sup>36</sup>. Thus, freeze-thaw has carry-over effects on wetland soil nitrogen in the early growing season and enhances N limitation in wetland ecosystem.

Studies have illustrated that the freeze-thaw does not carry over to the subsequent seasons<sup>37</sup> because of sampling time differences<sup>29</sup> or other environmental factors that offset the freeze-thaw effects<sup>19</sup>. For middle or high latitudes and high-altitude regions, freeze-thaw is an important natural stress influencing wetland ecological processes and functions, although it occurs only a few times throughout the year<sup>24,30</sup>. As one of the most productive ecosystems<sup>31</sup>, the fact that freeze-thaw has carry-over effects on soil nutrients and microbial communities in wetland suggests that studies may underestimate the persistence and influence of freeze-thaw ecological effects. However, this important discovery was proven through a simulated freeze-thaw experiment in this study, which requires further field studies to investigate in nature and incorporate the more environmental factors induced by climate change.

**Wetland plant changes its sprouting strategy to adapt to the enhanced nitrogen limitation caused by the freeze-thaw's carry-over effects.** Our experimental results showed that the freeze-thaw groups had a lower sprouting number and speed than the control groups, but there was no difference between the treatment and control groups at the end of the experiment. The ramet eco-physiological characteristics (Fv:Fm, TC in leaf, height, leaf number, and aboveground biomass) were lower in freeze-thaw groups than in the control groups, suggesting that freeze-thaw has carry-over effects of inhibiting sprouting and ramet growth. The cascade relationships among the inhibited sprouting and ramet growth, the decreased soil nitrogen, and the enhanced denitrification (Figs. 4 and 5 and Supplementary Fig. 10) suggest that there is a regulation and limitation of soil nitrogen on sprouting and ramet growth resulting from the freeze-thaw's carry-over effects on fueling denitrification, resultant nitrogen reduction, and intensified nitrogen limitation. First, nitrate, as an essential source of plant nitrogen and an environmental trigger regulating plant germination and growth, could lower abscisic acid levels, break seed dormancy, and prompt germination<sup>38</sup>. It has been proven that increased soil available nitrogen can prompt bud dormancy to break in many grass species<sup>39</sup>. The freeze-thaw's carry-over effects significantly reduced nitrate in soil in this study, resulting in a low-nitrate environment that enforced dormancy<sup>38</sup> and further delayed plant sprouting and early growth. Second, nitrogen, as one of the important components of DNA, RNA, proteins, and enzymes, is critical for plant growth and development. Studies have documented that low soil nitrogen availability is the major nutrient factor limiting plant growth in N-limited ecosystems<sup>40</sup>. Therefore, the enhanced N limitation caused by the freeze-thaw's carry-over effects further limits ramet growth. Furthermore, we summarized this cascade relationship by using a conceptualized bullet model (Fig. 5).

The differences in plant sprouting between the freeze-thaw and control groups during the experiment disappeared at the end of the experiment. We speculate that plants adapt to nitrogen-limiting stress by altering sprouting strategies, because we found different sprouting-time patterns between treatments (Fig. 5b, c): during the early sprouting period, freeze-thaw groups had significantly lower sprouting number and speed than control groups; over time, the sprouting speed in freeze-thaw groups was gradually higher than that in control groups; finally, the sprouting number in freeze-thaw groups did not differ from control groups. The significant positive relationship between soil nitrogen and sprouting indicated that the reduced soil nitrogen under the freeze-thaw's carry-over effects might enhance the intraspecific

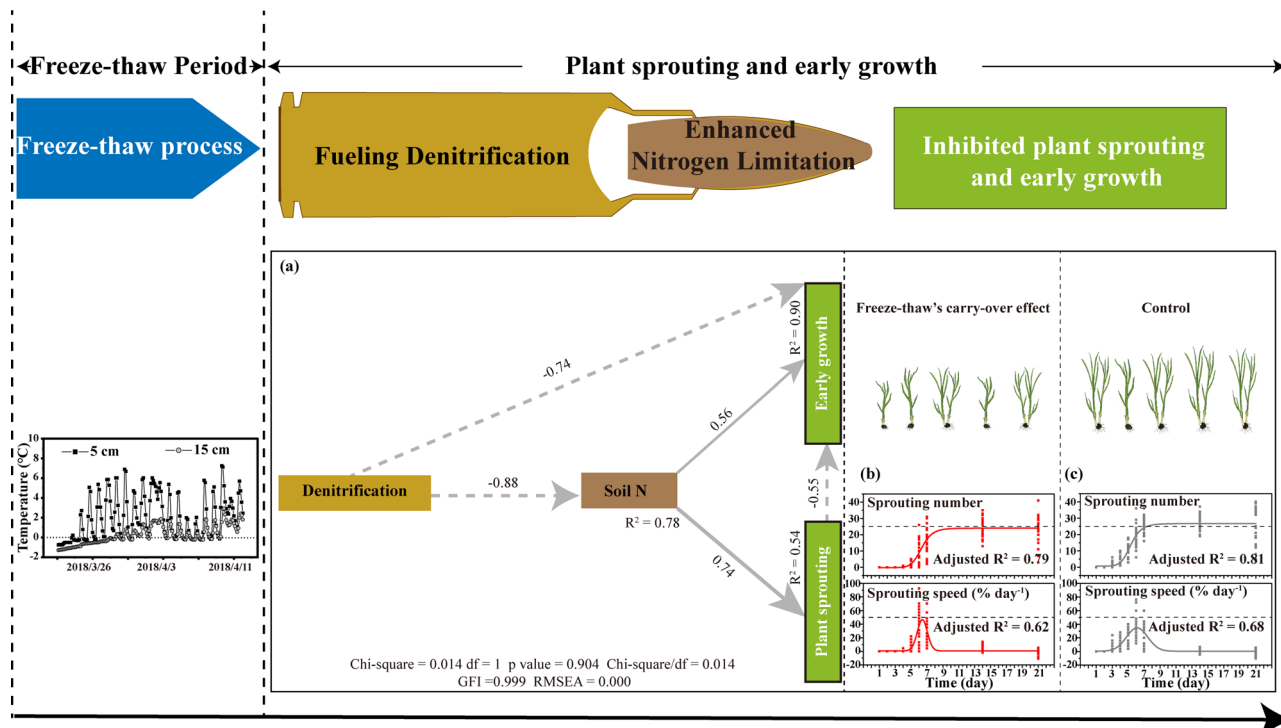


**Fig. 5 Conceptual representation of the cascade relationship of soil microbes, soil nutrients, and plant sprouting and early growth under the freeze-thaw's carry-over effects.** **a** The result of the SEM (dashed and solid lines represent negative and positive relationships, respectively; R<sup>2</sup> represents the explained variation; the values on the lines indicate standardized path coefficients; paths with significant coefficients (p < 0.05) are shown); **b, c** the sprouting-time pattern.

competition for nitrogen (Fig. 5a). Under resource limitation, inhibited germination could alleviate intraspecific competition for resources<sup>41,42</sup>. Similar to the sprouting-time patterns mentioned above, when portions of plants are resistant to nitrogen limitation stress, the remaining propagules begin to sprout at a high speed to increase individual numbers, indicating a strategy for plants to efficiently use resources and adapt to resource scarcity in resource-limited environments.

Soil temperature is also a key environmental factor influencing plant dormancy and sprouting<sup>38</sup>, however, it is not the main reason for differences in sprouting between treatments in this study. Although soil temperatures during freeze-thaw period were different between treatments (Supplementary Fig. 4 and Supplementary Table 3), the lowest soil temperature was very mild (-0.38 ± 0.05°C), indicating that plant cell damage might not have occurred. Furthermore, all of the plants in this study sprouted and grew at the same environmental temperature. Before freeze-thaw treatment, all samples were incubated at 6 °C for 1 week; thereby, freeze-thaw cycles were initiated and ended at the thaw phase (Supplementary Fig. 1b). Therefore, although the soil temperature lags behind the air temperature, the soil temperature of the freeze-thaw groups was the same as that of the control groups within several hours after the last freeze-thaw cycle. In addition, because *Scirpus planiculmis* sprouts at average air temperatures above 10 °C<sup>43</sup> and its base temperature is 6.2 °C<sup>44</sup>, they did not sprout until they were transferred to the greenhouse for sprouting and early growth, where the air temperature ranged from 16 °C to 30 °C.

Plant sprouting, including seed germination and bud sprouting, is an important stage in plant life cycles and environmental fitness<sup>17,45</sup>, determining a population's ability to cope with climate change<sup>46</sup>. Changes in within-species germination strategies are crucial for maintaining population persistence in a rapidly changing climate<sup>18</sup>. Our study indicated that plant

adjusted its sprouting strategy to reduce the inhibitory impact of the freeze-thaw's carry-over effects on plant sprouting and early growth to ensure the population's stability and survival. Studies have been conducted on plant germination strategies under random environmental disturbance events such as frost<sup>47</sup>. However, for seasonal biotic stress, there is little understanding of plants' adaptive strategies responses to freeze-thaw changes. Therefore, whether previous studies on environmental stress overemphasized extreme climatic events while ignoring seasonal abiotic stress is an issue worthy of attention in future research.

**The existence of flooding alleviates the freeze-thaw's carry-over effects.** Furthermore, we discovered that flooding can trade-off the freeze-thaw's carry-over effects on soil nutrients and alleviate enhanced nitrogen limitation. Our experimental results showed that the freeze-thaw's carry-over effects on most plant traits, soil nutrients, and microbial attributes were in the opposite direction from the flooding effects, with the influence of flooding or the freeze-thaw's carry-over effects being greater than their interaction (Supplementary Fig. 11). Moreover, the flooding groups had higher soil nitrogen than non-flooding groups (Supplementary Fig. 5). First, the existence of flooding attenuates soil denitrification. Our experimental results showed that denitrification, resulting in soil nitrogen loss, was weaker in the flooding groups than in non-flooding groups. The main N-cycling metabolic processes in this study were organic nitrogen biosynthesis and biodegradation and denitrification, with flooding groups having weaker denitrification and organic nitrogen biodegradation than non-flooding groups (Fig. 3). The non-flooding groups should have higher soil oxygen content than the flooding groups due to the barrier effect of flooding on oxygen, which would cause higher mineralization of organic matter and, further, provide more energy and substrates to enhance denitrification (Fig. 3, Supplementary Fig. 5). Furthermore, the soil N:P ratio was

significantly lower in the non-flooding groups than in the flooding groups (Supplementary Fig. 5), indicating the relative alleviation of phosphorus limitation and leading to the enhancement of denitrification<sup>48,49</sup>. Second, the existence of flooding alleviated the influence of air temperature fluctuations on soil, and weakened the freeze-thaw's intensity. Compared to the non-flooding groups, the flooding groups had a smaller temperature fluctuation, a shorter freezing period, and lower variations in  $\text{NO}_3^-$ -N content and microbial community attributes between the freeze-thaw and control groups (Fig. 2, Supplementary Figs. 5 and 6, Supplementary Table 2, and Supplementary Table 3). Besides, the differential microorganisms, which accounted for more than 70% of the total relative abundance (Supplementary Fig. 8), had no difference between the freeze-thaw and control groups under the flooding conditions (Supplementary Fig. 7). Consequently, we speculated that the alleviated freeze-thaw effects by flooding had weaker carry-over effects on the soil microbial communities and nitrogen metabolism and further reduced the nitrogen limitation. Thus, wetland plant sprouting under the freeze-thaw treatment was earlier and faster in the flooding groups than in the non-flooding groups (Fig. 1).

However, continuous flooding was detrimental to plant growth and survival during the early growth phase. Because the number of healthy ramets (with a green appearance), the number of ramets with a height over 10 cm, Fv:Fm, leaf number, leaf width, height, and aboveground biomass in the flooding groups were lower than those in the non-flooding groups (Supplementary Fig. 2). Moreover, the increased stem diameter and higher S:L ratio under the flooding conditions further verified the flooding stress on ramets (Supplementary Fig. 2). Most wetland plants have an adaptive trait, aerenchyma, in their stems, and an increased stem diameter could enhance the plant's gas transport capacity<sup>50</sup>. Furthermore, a higher S:L ratio implies that more sources are utilized for stem development, which is beneficial for increasing plant height and air contact<sup>51</sup>. Therefore, increased stem diameter and a higher S:L ratio could help ramets survive under anaerobic and anoxic stress caused by flooding. Hydrologic conditions are extremely crucial for maintaining wetland ecological structures and functions<sup>31</sup>. Consequently, winter precipitation and early spring snow-melting could be the determining factors regulating plant population establishment and community construction in wetlands, according to the disruption of flooding on freeze-thaw's effects.

Altogether, we clarified the freeze-thaw's carry-over effects on wetland soil and plant and built up the cascade relationship of soil microbes-soil nutrients-plant sprouting and early growth. The most interesting discovery is that the freeze-thaw's carry-over effects altered the wetland plant sprouting strategy by fueling denitrification. Besides, we found that flooding could alleviate the freeze-thaw's carry-over effects mentioned above. Under climate change, the fluency, occurrence time, and duration of the freeze-thaw cycles may change as a result of fluctuations in winter snow cover, temperature, and precipitation, altering the nutrient limitation and cycles of wetlands in mid-to-high latitudes and high altitudes; this will further prompt or inhibit the sprouting and early growth of wetland plants, change the competition ability of wetland plants, and thereby reshape the plant community structure and succession in wetlands. Our research enriches the theoretical research on wetland ecological processes and functions, which will aid in the accurate assessment of climate change's effects on wetlands. It can also be applied to nitrogen management and productivity improvements in wetlands.

## Methods

**Material collection and preparation.** The Momoge wetland (45° 53' 36.06" N, 123° 37' 31.97" E) is located in the western Songnen Plain, a typically seasonally

frozen region, which undergoes soil freeze-thaw in spring and autumn annually. Soil melting starts from late March to early April, whereas freezing starts from mid-November<sup>52</sup>. The mean annual temperature in this area is 4.2 °C, with a 137-day frost-free period, and 76% of the annual precipitation is mainly concentrated from July to September<sup>53</sup>. The dominant marsh plants are *Scirpus planiculmis*, *Schoenoplectus nipponicus*, and *Phragmites australis*. According to the Harmonized World Soil Database Viewer (Version 1.2)<sup>54</sup>, the soil types include Phaeozems, Gleysols, Arenosols, and Chernozems. The organic matter content of soil ranges from 4 g kg<sup>-1</sup> to 91 g kg<sup>-1</sup>,<sup>55</sup> total nitrogen ranges from 0.27 g kg<sup>-1</sup> to 0.87 g kg<sup>-1</sup>, the pH varies from 7.99 to 9.67,<sup>56</sup> and the Momoge wetland is a mineral wetland.

*S. planiculmis* is the dominant and important constructive species in the Momoge wetland, as well as a typical tuber-forming perennial herb that is widespread in grassland, wetland, and rice fields throughout Eurasia<sup>57,58</sup> and that can occasionally produce new individuals by seed germination<sup>59</sup>. *S. planiculmis* usually sprouts when the average air temperature is over 10 °C from early May to mid-May and blooms at the end of May<sup>43</sup>. In addition, 0–10 cm flooding is a suitable condition for sprouting of *S. planiculmis* and –5–10 cm is good for its early growth<sup>57,60</sup>. Tuber sprouting is one of the modes of clonal growth that is the main propagation mode for wetland plants<sup>61</sup>. Therefore, *S. planiculmis* is appropriate for solving the scientific problems raised in this study, and the conclusions are applicable to the majority of wetland plants that produce new individuals mainly by clone propagation.

Tubers of *S. planiculmis* and soil were collected from the Momoge wetland and transported to the Northeast Institute of Geography and Agroecology in June 2017. Before starting the experiment, we conserved healthy and similar-sized tubers in a 4 °C incubator, picked out stones and roots from the soil, and blended the soil into a homogeneous medium.

**Experimental designs.** A temperature-controlling simulation experiment with wetland soil and plant was performed with two freeze-thaw conditions (freeze-thaw, control) and two flooding conditions (0 cm: non-flooding, 10 cm: flooding). The soil moisture of non-flooding was saturated, and the soil was weighed and watered every day to maintain a constant soil moisture. Before we started the experiment, 25 tubers were planted in one pot (non-flooding: 14 cm in length, 17 cm in width, and 25 cm in height; flooding: 14 cm in length, 17 cm in width, and 35 cm in height) with 20 cm depth soil, and 48 pots in all treatments: 2 freeze-thaw conditions × 2 flooding conditions × 12 replicates (Supplementary Fig. 1b). Before freeze-thaw treatment, we incubated samples at 6 °C for 1 week. Freeze-thaw treatment was performed in an environmental test chamber (Rosenyi, Tinghua, Tianjin), a device that could set the temperatures for simulating the freeze-thaw cycles. The freeze-thaw cycles were set based on soil temperature changes and freeze-thaw duration (approximately lasting 18 days) during the spring freeze-thaw in 2018, which were recorded using temperature data loggers (HOBO TidbiT v2 UTBI-001, Onset, USA) and are shown in Supplementary Fig. 1a. Because the historical mean air temperature for the first day of freeze-thaw period (March 23) in 2018 ranged from –7 to 7 °C (<http://forecast.weather.com.cn/town/weathern/101060604013.shtml?from=map>), and the mean air temperature for the month ranged from –9 to 5 °C (<https://lishi.tianqi.com/zhenlai/201803.html>), we simulated the air temperature to fluctuate between –7 and 7 °C. More specifically, for freeze-thaw treatment, we set the air temperature to fluctuate from –7–7 °C every 24 h (one freeze-thaw cycle) with 4 h at –7 °C and 4 h at 7 °C, whereas the control treatment was still incubated at 6 °C until the simulation of freeze-thaw finished (Supplementary Fig. 1b). Furthermore, in one freeze-thaw cycle, we set –2 °C to –7 °C at 2 h and 2 °C to 7 °C at 2 h to simulate the slow temperature drop or rise in nature. After 18 days of freeze-thaw cycles, all treatments were incubated at 6 °C for 1 week and then moved to the greenhouse with semitransparent baffles for sprouting and early growth for 21 days, where the air temperature ranged from 16 °C to 30 °C, the humidity was 40–50%, and the light was close to natural light. The day that all the samples were moved to the greenhouse was considered the first day of sprouting because *S. planiculmis* begins sprouting when the average air temperature is over 10 °C and its base temperature is 6.2 °C<sup>44</sup>, and the sprouting and early growth phase lasted 21 days because it sprouts from early May to mid-May in the Momoge wetland. Soil temperatures at 5 cm depth during the freeze-thaw period were recorded using temperature data loggers (HOBO TidbiT v2 UTBI-001, Onset, USA) for 3 replicates per treatment.

**Plant eco-physiological characteristics and soil nutrients.** During sprouting and early growth, we recorded the numbers of sprouts and ramets as the sprouting number every day during the first week, and then, once per week. Furthermore, we calculated the sprouting percentage per day as the sprouting speed based on the recorded sprouting number. After 3 weeks, we recorded height, leaf number, stem diameter, and leaf width, and measured the chlorophyll fluorescence parameter (Fv:Fm) using a fluorometer (PAM 2500, Walz, Germany). The number of ramets with a green appearance and the number of ramets with a height of over 10 cm were also counted. Then, leaves and stems were collected separately and air-dried at 105 °C for 15 min and at 65 °C until reaching a constant weight. Parts of dried leaves and stems were weighed and calculated for S:L ratio and aboveground biomass, and the remaining parts were used for measuring TN, TC, TP, TS, and N:P ratio. To reduce measurement errors, height, leaf number, stem diameter, leaf width, S:L ratio, and aboveground biomass were randomly measured from three

individuals in one pot as one replicate. In addition, parts of soil samples in pots were collected and frozen in liquid nitrogen and stored at  $-80^{\circ}\text{C}$  before high-throughput sequencing and metagenomic sequencing, and the remaining parts were collected, air dried, and sieved (0.149 mm) for measuring TN, TON,  $\text{NH}_4^{+}\text{-N}$ ,  $\text{NO}_3^{-}\text{-N}$ , TC, TP, and N:P ratio. All measurements in this study were taken from distinct samples.

TP and TS in plants and TP in soil were measured by inductively coupled plasma atomic emission spectrometry (ICP-AES; ICPS-7500, Shimadzu Corporation, Japan) after digestion (plant:  $\text{HNO}_3\text{-HClO}_4$  digestion method; soil:  $\text{HNO}_3\text{-HF-HClO}_4$  digestion method)<sup>62,63</sup>. Following a previous study<sup>21</sup>,  $\text{NH}_4^{+}\text{-N}$  and  $\text{NO}_3^{-}\text{-N}$  in soil were measured by colorimetric analyses after being extracted by 2 M KCl, TN was measured by flow analyses (Smarchem300, AMS, Italia) after Kjeldahl digestion, and TON was calculated according to the contents of TN,  $\text{NH}_4^{+}\text{-N}$ , and  $\text{NO}_3^{-}\text{-N}$ . The TC of the plant and soil was measured by the potassium dichromate heating method<sup>24</sup>.

**High-throughput sequencing analysis.** Following the manufacturer's protocol, the total DNA in soil samples was extracted using a Power Soil DNA Isolation Kit (MO BIO Laboratories, USA). The 16S rRNA gene in the V3-V4 region was amplified using DNA barcoding primers (338F: 5'-ACTCCTACGGGAGG-CAGCA-3'; 806R: 5'-GGACTACHVGGGTWTCTAAT-3'). A total volume of 20  $\mu\text{L}$  PCR amplification was performed including 13.25  $\mu\text{L}$   $\text{H}_2\text{O}$ , 10  $\times$  PCR ExTaq Buffer 2.0  $\mu\text{L}$ , DNA template (100 ng/mL) 0.5  $\mu\text{L}$ , prime1 (10 mmol/L) 1.0  $\mu\text{L}$ , prime2 (10 mmol/L) 1.0  $\mu\text{L}$ , dNTP 2.0  $\mu\text{L}$ , and ExTaq (5 U/mL) 0.25  $\mu\text{L}$ . Then, 1.0% agarose gel electrophoresis method was conducted to purify and recover the amplified products. Finally, library construction and high-throughput sequencing analysis were performed using the Illumina HiSeq platform (paired-ends) at Beijing Biomarker Technologies Co., Ltd.

The paired-end reads of each sample were spliced using FLASH<sup>64</sup> (version 1.2.11) and were filtered and clustered via Trimmomatic<sup>65</sup> (version 0.33). Furthermore, the possible chimeras were identified and removed by UCHIME<sup>66</sup> (version 8.1) to obtain high-quality sequences. The denoised sequences were clustered (USEARCH<sup>67</sup>, version 10.0) and regarded as an OTU at a similarity of more than 97%. Finally, by searching against the Silva database<sup>68</sup> (version 128) with the RDP classifier<sup>69</sup> (version 2.2, confidence threshold: 0.8), taxonomy was assigned to all OTUs.

**Metagenomic sequencing.** Three soil samples from each treatment were randomly selected for metagenomic sequencing. Soil total DNA was extracted in the same way as for high-throughput sequencing analysis. Metagenome sequencing was performed at Beijing Biomarker Technologies Co., Ltd. using Illumina high-throughput sequencing and small fragment libraries were constructed with the paired-end method for sequencing.

The low-quality sequences in sequenced raw reads were filtered to obtain clean reads for subsequent bioinformatics analysis using Trimmomatic<sup>65</sup> (version 0.33, parameters: LEADING:3 TRAILING:3 SLIDINGWINDOW:50:20 MINLEN:100). The metagenome assembly was performed using MEGAHIT<sup>70</sup> (version 1.1.2), and the contig sequences that were shorter than 300 bp were filtered out. Then, the assembly results were evaluated by employing QUAST<sup>71</sup> (version 2.3). Genes in assembled contigs were predicted by using MetaGeneMark<sup>72</sup> (version 3.26) with default settings. Finally, a nonredundant gene set was constructed by removing redundant sequences via cd-hit<sup>73</sup> (version 4.6.6) at 95% similarity and 90% coverage. In addition, genes in the nonredundant gene set were used to search against the KEGG database, the genes in KEGG with the highest similarity were chosen, and associated protein functional annotations were obtained (Diamond, version 0.9.29,  $E$  value  $< 1e-5$ )<sup>74</sup>.

To investigate microbial nitrogen metabolism under the carry-over effects of freeze-thaw, we selected the N-cycling genes from the annotation results to recalculate their relative abundance and alpha and beta diversity. Furthermore, some selected key N-cycling genes (Supplementary Table 4) were used to calculate the genetic potential of N-cycling metabolic processes according to the method in previous studies<sup>75-77</sup>.

**Statistical analysis.** Data, including plant sprouting and eco-physiological characteristics, soil nutrients, alpha diversity of microbial community and N-cycling genes, and genetic potential of N-cycling metabolic processes, were examined for normality (Shapiro-Wilk tests) and homogeneity (Levene's Test) across treatments before statistical analysis. Two-way ANOVA was used to test the differences between treatments for normal and homogeneous data, and aligned ranks transformation ANOVA was used for nonnormal or nonhomogeneous data, including Simpson's diversity index of OTU, stem diameter, leaf width, TS (stem), TN (stem), TN (leaf), TN (soil), TC (leaf),  $\text{NH}_4^{+}\text{-N}$ , TON, leaf number, ramet number (a height of over 10 cm, a green appearance), N:P ratio (plant), N:P ratio (soil), genetic potential of dissimilatory nitrate reduction, sprouting number (day 3, day 4, day 5, day 21), and sprouting speed (day 3, day 4, day 5, day 6, day 21). Then,  $p < 0.05$  was used to assign significant differences. Tukey's post-hoc analysis was performed when interaction effects existed between the flooding and the freeze-thaw's carry-over effects. The effect size ( $\eta^2$  and Cohen's  $d$ ) was calculated based on the methods of Kay<sup>78</sup> and Mangiafico<sup>79</sup>. The above statistical analyses were carried out using stats package<sup>80</sup>, car package<sup>81</sup>, ARTool package<sup>82-84</sup> and emmeans package<sup>85</sup> in R version 4.0.2 (<https://www.r-project.org>), and graphics were produced with the ggplot2 R package<sup>86</sup>. To analyze the effect of flooding and the carry-over effects

of freeze-thaw on plant sprouting, including sprouting number and sprouting speed, we used a repeated measures analysis implemented with a generalized linear mixed model in SPSS software (version 22.0, IBM Corp, USA). According to the data distribution, we tried several methods to perform a nonlinear curve fit to investigate the sprouting-time pattern by using OriginPro 2021 (Origin Lab Corp., USA), and the fits with the greatest adjusted  $R^2$  and smallest reduced Chi-Sqr were selected under the different treatments.

To determine the differential microorganisms, linear discriminant analysis effect size (LEfSe) analysis was performed using BMKCloud (<http://www.biocloud.net>). The beta diversity of N-cycling functional genes and the microbial community (OTU level) was calculated by using PCoA based on Bray-Curtis distance in the vegan R package<sup>87</sup>, and its significance among treatments was analyzed by PERMANOVA. Furthermore, pairwise comparisons with  $p$ -values adjusted (Bonferroni correction) based on PERMANOVA results were performed when the interaction effects existed between flooding and the carry-over effects of freeze-thaw.

A partial Mantel test and Spearman correlation analysis were performed using the vegan R package<sup>87</sup> and the psych R package<sup>88</sup> to investigate the relationship between plant eco-physiological characteristics, soil nutrients, and microbial community attributes, including microbial community composition and nitrogen metabolism. Then, db-RDA and VPA were conducted to explore the relationship between soil nitrogen (TN,  $\text{NH}_4^{+}\text{-N}$ ,  $\text{NO}_3^{-}\text{-N}$ , TON, and N:P ratio) and N-cycling metabolic processes in the vegan R package<sup>87</sup>. The variables were chosen using a forward selection method to eliminate colinear variables and limit overfitting before analyzing the db-RDA and VPA. The correlation analysis results were drawn by using the corplot R package<sup>89</sup>, and the db-RDA and VPA results were drawn by using ggplot2<sup>86</sup>. Finally, SEM was conducted to confirm the cascade relationship between N-cycling metabolic processes, soil nitrogen, plant sprouting, and early growth (AMOS 24, Amos Development Corporation, Chicago, IL, USA). Based on the results of db-RDA and VPA, denitrification was selected to construct the model rather than all N-cycling metabolic processes. Plant eco-physiological characteristics that were significantly influenced by flooding and the freeze-thaw's carry-over effects, including the S:L ratio, height, leaf number, stem diameter, leaf width, aboveground biomass, Fv:Fm, the number of ramets that reach a height of over 10 cm or with a green appearance, TP, TS, TN in leaves and stems, and TC in leaves, were selected to indicate the plant early growth. The sprouting number was chosen to represent plant sprouting in this model because it can reflect the change in sprouting speed and total number of ramets. To reduce the variables in SEM, we used PC1 in principal component analysis (PCA) to replace the datasets of soil nitrogen, plant sprouting and early growth (Supplementary Table 5), which were calculated by using OriginPro 2021 (Origin Lab Corp., USA). The models were fitted using the maximum likelihood (ML) method, and the best-fit model was examined using the  $p$  value, the ratio of chi-square and degrees of freedom ( $\chi^2/df$ ), goodness-of-fit index (GFI) and the root mean squared error of approximation (RMSEA) tests. Paths with the least impact on  $\chi^2$  and the least significance were removed for simplicity, and models were re-estimated until all of the paths left in the model were significant.

**Reporting summary.** Further information on research design is available in the Nature Portfolio Reporting Summary linked to this article.

## Data availability

Metagenomic sequencing data reported in this paper have been deposited in the Genome Sequence Archive (Genomics, Proteomics & Bioinformatics 2021) in National Genomics Data Center (Nucleic Acids Res 2021), China National Center for Bioinformation/Beijing Institute of Genomics, Chinese Academy of Sciences (GSA: CRA007175) that are publicly accessible at: <https://ngdc.cncb.ac.cn/gsa/browse/CRA007175>. 16S rRNA gene sequences were deposited to the National Center for Biotechnology Information (NCBI) under the project accession number PRJNA847345 and publicly accessible at: <https://www.ncbi.nlm.nih.gov/bioproject/PRJNA847345>. The remaining data including soil nutrients, plant eco-physiological characteristics, and soil temperatures were deposited on Figshare (<https://doi.org/10.6084/m9.figshare.22015319.v2>).

Received: 4 September 2022; Accepted: 16 February 2023;

Published online: 28 February 2023

## References

- Campbell, J. L. & Laudon, H. Carbon response to changing winter conditions in northern regions: current understanding and emerging research needs. *Environ. Rev.* **27**, 545–566 (2019).
- Groffman, P. M. et al. Effects of mild winter freezing on soil nitrogen and carbon dynamics in a northern hardwood forest. *Biogeochemistry* **56**, 191–213 (2001).
- Song, C. et al. Large methane emission upon spring thaw from natural wetlands in the northern permafrost region. *Environ. Res. Lett.* **7**, 034009 (2012).

4. Chen, H. et al. Methane emissions during different freezing-thawing periods from a fen on the Qinghai-Tibetan Plateau: Four years of measurements. *Agric. Ecosyst. Environ.* **297**, 108279 (2021).
5. Bao, T., Xu, X., Jia, G., Billesbach, D. P. & Sullivan, R. C. Much stronger tundra methane emissions during autumn freeze than spring thaw. *Glob. Chang. Biol.* **27**, 376–387 (2021).
6. Yu, J. et al. Enhanced net formations of nitrous oxide and methane underneath the frozen soil in Sanjiang wetland, northeastern China. *J. Geophys. Res.* **112**, D07111 (2007).
7. Kreyling, J., Peršoh, D., Werner, S., Benzenberg, M. & Wöllecke, J. Short-term impacts of soil freeze-thaw cycles on roots and root-associated fungi of *Holcus lanatus* and *Calluna vulgaris*. *Plant Soil* **353**, 19–31 (2012).
8. Min, K., Chen, K. & Arora, R. Effect of short-term versus prolonged freezing on freeze-thaw injury and post-thaw recovery in spinach: Importance in laboratory freeze-thaw protocols. *Environ. Exp. Bot.* **106**, 124–131 (2014).
9. Kennedy, A. Photosynthetic response of the Antarctic moss *Polytrichum alpestre* Hoppe to low temperatures and freeze-thaw stress. *Polar Biol.* **13**, 271–279 (1993).
10. Sanders-DeMott, R., Sorensen, P. O., Reinmann, A. B. & Templer, P. H. Growing season warming and winter freeze-thaw cycles reduce root nitrogen uptake capacity and increase soil solution nitrogen in a northern forest ecosystem. *Biogeochemistry* **137**, 337–349 (2018).
11. Vankoughnett, M. R. & Henry, H. A. L. Soil freezing and N deposition: transient vs. multi-year effects on extractable C and N, potential trace gas losses and microbial biomass. *Soil Biol. Biochem.* **77**, 170–178 (2014).
12. Kreyling, J., Beierkuhnlein, C., Pritsch, K., Schloter, M. & Jentsch, A. Recurrent soil freeze-thaw cycles enhance grassland productivity. *New Phytol.* **177**, 938–945 (2008).
13. Song, Y., Zou, Y., Wang, G. & Yu, X. Altered soil carbon and nitrogen cycles due to the freeze-thaw effect: a meta-analysis. *Soil Biol. Biochem.* **109**, 35–49 (2017).
14. Vankoughnett, M. R. & Henry, H. A. L. Soil freezing and N deposition: transient vs multi-year effects on plant productivity and relative species abundance. *New Phytol.* **202**, 1277–1285 (2014).
15. Luan, Z. & Cao, H. Response of fine root growth and nitrogen and phosphorus contents to soil freezing in *Calamagrostis angustifolia* wetland, Sanjiang Plain, Northeast China. *J. Food Agric. Environ.* **10**, 1495–1499 (2012).
16. Garcia, M. O. et al. Soil microbes trade-off biogeochemical cycling for stress tolerance traits in response to year-round climate change. *Front. Microbiol.* **11**, 616 (2020).
17. Tang, H., Bai, J., Chen, F., Liu, Y. & Lou, Y. Effects of salinity and temperature on tuber sprouting and growth of *Schoenoplectus nipponicus*. *Ecosphere* **12**, e03448 (2021).
18. Satyanti, A., Guja, L. K. & Nicotra, A. B. Temperature variability drives within-species variation in germination strategy and establishment characteristics of an alpine herb. *Oecologia* **189**, 407–419 (2019).
19. Harrison, J. L., Schultz, K., Blagden, M., Sanders-DeMott, R. & Templer, P. H. Growing season soil warming may counteract trend of nitrogen oligotrophication in a northern hardwood forest. *Biogeochemistry* **151**, 139–152 (2020).
20. Semenchuk, P. R. et al. Deeper snow alters soil nutrient availability and leaf nutrient status in high Arctic tundra. *Biogeochemistry* **124**, 81–94 (2015).
21. Song, Y., Zou, Y., Wang, G. & Yu, X. Stimulation of nitrogen turnover due to nutrients release from aggregates affected by freeze-thaw in wetland soils. *Phys. Chem. Earth* **97**, 3–11 (2017).
22. Keith, D. A., Rodoreda, S. & Bedward, M. Decadal change in wetland-wetland boundaries during the late 20th century reflects climatic trends. *Glob. Chang. Biol.* **16**, 2300–2306 (2010).
23. Wang, J., Song, C., Hou, A. & Xi, F. Methane emission potential from freshwater marsh soils of Northeast China: response to simulated freezing-thawing cycles. *Wetlands* **37**, 437–445 (2017).
24. Yu, X. et al. Wetland plant litter decomposition occurring during the freeze season under disparate flooded conditions. *Sci. Total Environ.* **706**, 136091 (2020).
25. Dong, X. et al. Variations in active layer soil hydrothermal dynamics of typical wetlands in permafrost region in the Great Hing'an Mountains, northeast China. *Ecol. Indic.* **129**, 107880 (2021).
26. Li, Y. et al. Freeze-thaw cycles increase the mobility of phosphorus fractions based on soil aggregate in restored wetlands. *CATENA* **209**, 105846 (2022).
27. Song, C., Zhang, J., Wang, Y., Wang, Y. & Zhao, Z. Emission of CO<sub>2</sub>, CH<sub>4</sub> and N<sub>2</sub>O from freshwater marsh in northeast of China. *J. Environ. Manage.* **88**, 428–436 (2008).
28. Wang, G., Liu, J., Zhao, H., Wang, J. & Yu, J. Phosphorus sorption by freeze-thaw treated wetland soils derived from a winter-cold zone (Sanjiang Plain, Northeast China). *Geoderma* **138**, 153–161 (2007).
29. Ji, X., Liu, M., Yang, J. & Feng, F. Meta-analysis of the impact of freeze-thaw cycles on soil microbial diversity and C and N dynamics. *Soil Biol. Biochem.* **168**, 108608 (2022).
30. Ren, J. et al. Shifts in soil bacterial and archaeal communities during freeze-thaw cycles in a seasonal frozen marsh, Northeast China. *Sci. Total Environ.* **625**, 782–791 (2018).
31. Mitsch, W. J. & Gosselink, J. G. *Wetlands*. 5th edn (Wiley, Hoboken, New Jersey, 2015).
32. Yu, X., Zou, Y., Jiang, M., Lu, X. & Wang, G. Response of soil constituents to freeze-thaw cycles in wetland soil solution. *Soil Biol. Biochem.* **43**, 1308–1320 (2011).
33. Sawicka, J. E., Robador, A., Hubert, C., Jørgensen, B. B. & Bruchert, V. Effects of freeze-thaw cycles on anaerobic microbial processes in an Arctic intertidal mud flat. *ISME J* **4**, 585–594 (2010).
34. Song, Y. *The Freeze-thaw Effect On Soil Mineralization Between Various Moisture States Of Wetlands*. Master of Natural Science thesis (Northeast Institute of Geography and Agroecology, Chinese Academy of Sciences, 2017).
35. Mason, R. E. et al. Evidence, causes, and consequences of declining nitrogen availability in terrestrial ecosystems. *Science* **376**, eabh3767 (2022).
36. Koerselman, W. & Meuleman, A. F. M. The vegetation N:P ratio: a new tool to detect the nature of nutrient limitation. *J. Appl. Ecol.* **33**, 1441–1450 (1996).
37. Yang, K. et al. Immediate and carry-over effects of increased soil frost on soil respiration and microbial activity in a spruce forest. *Soil Biol. Biochem.* **135**, 51–59 (2019).
38. Lambers, H., Chapin, F. S. I. & Pons, T. L. *Plant Physiological Ecology*. 2nd edn (Springer, 2008).
39. Ott, J. P., Klimešová, J. & Hartnett, D. C. The ecology and significance of below-ground bud banks in plants. *Ann. Bot.* **123**, 1099–1118 (2019).
40. Pedersen, E. P., Elberling, B. & Michelsen, A. Foraging deeply: depth-specific plant nitrogen uptake in response to climate-induced N-release and permafrost thaw in the High Arctic. *Glob. Chang. Biol.* **26**, 6523–6536 (2020).
41. Dyer, A.R. Maternal and sibling factors induce dormancy in dimorphic seed pairs of *Aegilops triuncialis*. *Plant Ecol.* **172**, 211–218 (2004).
42. Renne, I. J. et al. Eavesdropping in plants: delayed germination via biochemical recognition. *J. Ecol.* **102**, 86–94 (2014).
43. Li, H. *Eco-physiological Responding Characteristics of Scirpus Planiculmis on Coupling of Water Table Depths and Salinity in Momoge Wetland*. Master Dissertation thesis, University of Chinese Academy of Sciences (Northeast Institute of Geography and Agroecology, Chinese Academy of Sciences, 2013).
44. Yu, D. *Responses of Sprouting and Growth to Environmental Factors in Bolboschoenus Planiculmis*. Master Dissertation thesis (Harbin Normal University, 2022).
45. Zhang, C., Willis, C. G., Donohue, K., Ma, Z. & Du, G. Effects of environment, life-history and phylogeny on germination strategy of 789 angiosperms species on the eastern Tibetan Plateau. *Ecol. Indic.* **129**, 107974 (2021).
46. Hoyle, G. L. et al. Seed germination strategies: an evolutionary trajectory independent of vegetative functional traits. *Front. Plant Sci.* **6**, 731 (2015).
47. Mercer, K. L., Alexander, H. M. & Snow, A. A. Selection on seedling emergence timing and size in an annual plant, *Helianthus annuus* (common sunflower, Asteraceae). *Am. J. Bot.* **98**, 975–985 (2011).
48. Cui, Y. et al. Ecoenzymatic stoichiometry reveals microbial phosphorus limitation decreases the nitrogen cycling potential of soils in semi-arid agricultural ecosystems. *Soil Tillage. Res.* **197**, 104463 (2020).
49. Ye, Z. et al. Ecoenzymatic stoichiometry reflects the regulation of microbial carbon and nitrogen limitation on soil nitrogen cycling potential in arid agriculture ecosystems. *J. Soils Sediments* **22**, 1228–1241 (2022).
50. Pan, Y. et al. Drivers of plant traits that allow survival in wetlands. *Funct. Ecol.* **34**, 956–967 (2020).
51. Pezeshki, S. R. Wetland plant responses to soil flooding. *Environ. Exp. Bot.* **46**, 299–312 (2001).
52. Zheng, S. *Soil Water-heat Process and Nitrogen Transformation During Freezing and Thawing Period in Wetland of Momoge*. Master Dissertation thesis (Jilin Agricultural University, 2019).
53. An, Y., Gao, Y., Zhang, Y., Tong, S. & Liu, X. Early establishment of *Suaeda salsa* population as affected by soil moisture and salinity: implications for pioneer species introduction in saline-sodic wetlands in Songnen Plain, China. *Ecol. Indic.* **107**, 105654 (2019).
54. FAO/IIASA/ISRIC/ISS-CAS/JRC. Harmonized World Soil Database (version 1.2). (FAO, Rome, Italy and IIASA, Laxenburg, Austria, 2012).
55. Jiang, M., Lu, X., Xu, L. & Yang, Q. Estimation on benefit of latent soil nutrient in melmeg reserve wetlands. *J. Nat. Resour.* **20**, 279–285 (2005).
56. Wang, Y. & Zhang, S. The pH distribution and soil nutrient characteristic at different habitats—a case study of Momoge Wetland. *J. Anhui Agric. Sci.* **50**, 135–139 (2022).
57. Hao, M. *The Ecological Restoration Research on Momoge Scirpus Planiculmis Wetland*. Master Dissertation thesis, University of Chinese Academy of Sciences (Northeast Institute of Geography and Agroecology, Chinese Academy of Sciences, 2016).
58. Ma, H. et al. Effect of nitrate supply on the facilitation between two salt-marsh plants (*Suaeda salsa* and *Scirpus planiculmis*). *J. Plant. Ecol.* **13**, 204–212 (2020).

59. Liu, B. et al. Effects of burial depth and water depth on seedling emergence and early growth of *Scirpus planiculmis* Fr. Schmidt. *Ecol. Eng.* **87**, 30–33 (2016).
60. Zhang, L., Zhang, G., Li, H. & Sun, G. Eco-physiological responses of *Scirpus planiculmis* to different water-salt conditions in Momoge wetland. *Pol. J. Environ. Stud.* **23**, 1813–1820 (2014).
61. Sosnová, M., van Diggelen, R. & Klimešová, J. Distribution of clonal growth forms in wetlands. *Aquat. Bot.* **92**, 33–39 (2010).
62. Lu, R. *Analytical Methods of Soil Agrochemistry* (China Agricultural Science and Technology Press, 2000).
63. Bao, S. *Soil and Agricultural Chemistry Analysis*. 3 edn. (China Agriculture Press, 2000).
64. Magoc, T. & Salzberg, S. L. FLASH: fast length adjustment of short reads to improve genome assemblies. *Bioinformatics* **27**, 2957–2963 (2011).
65. Bolger, A. M., Lohse, M. & Usadel, B. Trimmomatic: a flexible trimmer for Illumina sequence data. *Bioinformatics* **30**, 2114–2120 (2014).
66. Edgar, R. C., Haas, B. J., Clemente, J. C., Quince, C. & Knight, R. UCHIME improves sensitivity and speed of chimera detection. *Bioinformatics* **27**, 2194–2200 (2011).
67. Edgar, R. C. UPARSE: highly accurate OTU sequences from microbial amplicon reads. *Nat. Methods* **10**, 996–998 (2013).
68. Quast, C. et al. The SILVA ribosomal RNA gene database project: improved data processing and web-based tools. *Nucleic Acids Res.* **41**, D590–D596 (2013).
69. Wang, Q., Garrity, G. M., Tiedje, J. M. & Cole, J. R. Naïve Bayesian classifier for rapid assignment of rRNA sequences into the new bacterial taxonomy. *Appl. Environ. Microbiol.* **73**, 5261–5267 (2007).
70. Li, D., Liu, C. M., Luo, R., Sadakane, K. & Lam, T. W. MEGAHIT: an ultra-fast single-node solution for large and complex metagenomics assembly via succinct *de Bruijn* graph. *Bioinformatics* **31**, 1674–1676 (2015).
71. Gurevich, A., Saveliev, V., Vyahhi, N. & Tesler, G. QUAST: quality assessment tool for genome assemblies. *Bioinformatics* **29**, 1072–1075 (2013).
72. Zhu, W., Lomsadze, A. & Borodovsky, M. Ab initio gene identification in metagenomic sequences. *Nucleic Acids Res.* **38**, e132 (2010).
73. Fu, L., Niu, B., Zhu, Z., Wu, S. & Li, W. CD-HIT: accelerated for clustering the next-generation sequencing data. *Bioinformatics* **28**, 3150–3152 (2012).
74. Buchfink, B., Xie, C. & Huson, D. H. Fast and sensitive protein alignment using DIAMOND. *Nat. Methods* **12**, 59–60 (2015).
75. Lauro, F. M. et al. An integrative study of a meromictic lake ecosystem in Antarctica. *ISME J* **5**, 879–895 (2011).
76. Shen, M. et al. Trophic status is associated with community structure and metabolic potential of planktonic microbiota in Plateau lakes. *Front. Microbiol.* **10**, 2560 (2019).
77. Kieft, B. et al. Microbial community structure-function relationships in Yaquina Bay estuary reveal spatially distinct carbon and nitrogen cycling capacities. *Front. Microbiol.* **9**, 1282 (2018).
78. Kay, M. *Effect Sizes with ART* (2021).
79. Mangiafico, S. S. *Summary and Analysis of Extension Program Evaluation in R, version 1.18.8* <https://rcompanion.org/handbook/> (2016).
80. R Core Team R: *A Language and Environment for Statistical Computing* (2020).
81. Fox, J. & Weisberg, S. *An R Companion to Applied Regression*. 3rd edn (Thousand Oaks, Sage, CA, 2019).
82. Kay, M., Elkin, L. A., Higgins, J. J. & Wobbrock, J. O. ARTool: Aligned Rank Transform for Nonparametric Factorial ANOVAs. R package version 0.11.1. <https://doi.org/10.5281/zenodo.594511> (2021).
83. Wobbrock, J. O., Findlate, L., Gergle, D. & Higgins, J. J. The aligned rank transform for nonparametric factorial analyses using only anova procedures. *29th Annual Chi Conference on Human Factors in Computing Systems (CHI 2011)*, p. 143–146. <https://doi.org/10.1145/1978942.1978963> (2011).
84. Elkin, L. A., Kay, M., Higgins, J. J. & Wobbrock, J. O. An aligned rank transform procedure for multifactor contrast Tests. *Proceedings of the ACM Symposium on User Interface Software and Technology (UIST 2021)*, p. 754–768. <https://doi.org/10.1145/3472749.3474784> (2021).
85. Lenth, R. V. *emmeans: Estimated Marginal Means, aka Least-Squares Means*. R package version 1.6.3. (2021).
86. Wickham, H. *ggplot2: Elegant Graphics for Data Analysis* (2016).
87. Oksanen, J. et al. *vegan: Community Ecology Package*. R package version 2.5-7 (2020).
88. Revelle, W. *psych: Procedures for Psychological, Psychometric, and Personality Research, Northwestern University, Evanston, Illinois, USA*, R package version 2.2.9 (2022).
89. Wei, T. & Simko, V. R package ‘*corrplot*’: Visualization of a Correlation Matrix (Version 0.90) (2021).

## Acknowledgements

This research was funded by the National Natural Science Foundation of China (grant numbers 42222102, 42171107), and the Professional Association of the Alliance of International Science Organizations (Grant No. ANSO-PA-2020-14).

## Author contributions

S.D. designed the research, conducted the experiment, performed data analysis, drafted the figures, and wrote the first draft of the manuscript. Y.Z. reviewed and edited the manuscript. X.Y. designed the research, reviewed, and edited the manuscript.

## Competing interests

The authors declare no competing interests.

## Additional information

**Supplementary information** The online version contains supplementary material available at <https://doi.org/10.1038/s43247-023-00718-4>.

**Correspondence** and requests for materials should be addressed to Xiaofei Yu.

**Peer review information** *Communications Earth & Environment* thanks Fujuan Feng and the other, anonymous, reviewer(s) for their contribution to the peer review of this work. Primary Handling Editor: Aliénor Lavergne.

**Reprints and permission information** is available at <http://www.nature.com/reprints>

**Publisher's note** Springer Nature remains neutral with regard to jurisdictional claims in published maps and institutional affiliations.



**Open Access** This article is licensed under a Creative Commons Attribution 4.0 International License, which permits use, sharing, adaptation, distribution and reproduction in any medium or format, as long as you give appropriate credit to the original author(s) and the source, provide a link to the Creative Commons license, and indicate if changes were made. The images or other third party material in this article are included in the article's Creative Commons license, unless indicated otherwise in a credit line to the material. If material is not included in the article's Creative Commons license and your intended use is not permitted by statutory regulation or exceeds the permitted use, you will need to obtain permission directly from the copyright holder. To view a copy of this license, visit <http://creativecommons.org/licenses/by/4.0/>.

© The Author(s) 2023